

Tuning of upper critical field anisotropy in $\text{Tb}_x\text{Y}_{1-x}\text{Ni}_2\text{B}_2\text{C}$

H. Bitterlich, W. Löser,^{*} G. Behr, S.-L. Drechsler, K. Nenkov,[†] G. Fuchs, K.-H. Müller, and L. Schultz
Leibniz-Institut für Festkörper- und Werkstoffforschung Dresden, D-01171 Dresden, Germany

(Received 1 February 2002; published 31 May 2002)

The effect of paramagnetic Tb ions on the superconducting upper critical field H_{c2} of $\text{Tb}_x\text{Y}_{1-x}\text{Ni}_2\text{B}_2\text{C}$ intermetallic compounds has been studied on bulk single crystals, which is an example of continuous tuning of anisotropic behavior of pseudoquaternary borocarbide compounds. With an increasing Tb content x both T_c and the upper critical field H_{c2} are reduced. Different from $\text{YNi}_2\text{B}_2\text{C}$ a reversed large anisotropy $H_{c2}^{[001]} > H_{c2}^{[100]}$ is induced by the in-plane magnetic moments of the Tb ions, which is emphasized by the higher magnetization in the [100] direction. The magnitude of the anisotropy depends on the concentration x and the magnetic coupling between the Tb ions, and exhibits a maximum at $x=0.2$. A theory is presented which explains the anisotropy of the upper critical field on the basis of magnetization measurements.

DOI: 10.1103/PhysRevB.65.224416

PACS number(s): 74.62.Dh, 74.25.Ha, 74.70.Dd

I. INTRODUCTION

The intermetallic $R\text{Ni}_2\text{B}_2\text{C}$ (R =rare earth or Y) borocarbide superconductors¹⁻³ are having an impact on the study of the interplay of superconductivity and magnetic ordering. Solid solutions of nonmagnetic (Y, Lu) and magnetic (Tm, Er, Ho, Dy, Tb, Gd) rare-earth ions provide a unique opportunity to tune the strength of the mechanism of magnetic pair breaking,⁴⁻⁶ and thus to make a detailed study of it. Single crystals are the basis for a determination of anisotropic physical properties⁷ which can lead to a deeper insight into the superconducting mechanism. In superconducting single-crystalline $\text{YNi}_2\text{B}_2\text{C}$ samples the upper critical field H_{c2} for $H \perp [001]$ exceeds that for $H \parallel [001]$.⁸ Even a small in-plane anisotropy $H_{c2}^{[100]}(T) > H_{c2}^{[110]}(T)$ was reported.⁹ For $\text{TmNi}_2\text{B}_2\text{C}$, $\text{HoNi}_2\text{B}_2\text{C}$, and $\text{ErNi}_2\text{B}_2\text{C}$ superconducting borocarbide single crystals, a large anisotropy of the upper critical field $H_{c2}(T)$ parallel and perpendicular to the c axis was revealed.⁷ The anisotropy is induced by an effective field caused by the sublattice magnetization of the magnetic rare-earth ions Tm, Ho, and Er, respectively. Moreover, $H_{c2}(T)$ in $\text{ErNi}_2\text{B}_2\text{C}$ and $\text{HoNi}_2\text{B}_2\text{C}$ is strongly reduced compared to the $H_{c2}(T)$ of the nonmagnetic $\text{YNi}_2\text{B}_2\text{C}$ which is associated with enhanced pair breaking induced by the magnetic ions.

This paper aims to attack the effect of dilute magnetic Tb ions on the upper critical field in pseudoquaternary $\text{Tb}_x\text{Y}_{1-x}\text{Ni}_2\text{B}_2\text{C}$ single crystals. These compounds display superconductivity over a wide composition range up to $x=0.4$, and permit a tuning of the strength of magnetic pair breaking over a wide range.⁶ The critical temperature T_c is reduced with increasing x . The $\text{TbNi}_2\text{B}_2\text{C}$ compound itself exhibits an incommensurate antiferromagnetic order below $T_N=15.5$ K, which may be described as a spin-density wave longitudinally polarized along the a axis.¹⁰ Magnetic order occurs for $x \geq 0.3$, which gives rise to a coexistence with superconductivity in compounds with $0.3 \leq x \leq 0.4$. From the complex anisotropic magnetic order of $\text{TbNi}_2\text{B}_2\text{C}$ a sizable anisotropy of the effective field parallel and perpendicular to the c axis may be expected in dilute $\text{Tb}_x\text{Y}_{1-x}\text{Ni}_2\text{B}_2\text{C}$ alloys.

II. EXPERIMENTAL DETAILS

Bulk $\text{Tb}_x\text{Y}_{1-x}\text{Ni}_2\text{B}_2\text{C}$ single crystals ($x=0, 0.1, 0.2, 0.3$, and 0.4) have been prepared by floating-zone melting. Details of the crystal preparation and characterization were described elsewhere.¹¹ Single-crystalline samples of $2 \times 2 \times 2$ -mm³ size were subjected to a special high-temperature homogenization treatment up to 1435 °C within a resistance furnace under a purified Ar atmosphere.¹² The nominal Tb fraction x of each crystal was confirmed by electron-beam microanalysis with an accuracy of $<5\%$. The orientation of single crystals was determined by the x-ray Laue back-scattering method. The differential ac susceptibility of the samples $\chi_{ac}(T)$ was determined using a Lakeshore model 7225 ac susceptometer at 133 Hz, and an ac-field amplitude of 1 Oe in the temperature range from 2 to 17 K and at several constant magnetic fields. The upper critical field H_{c2} was determined as the superconducting onset of the $\chi_{ac}(T)$ curves. Because of the cubic shape of the samples the demagnetization factor for the different crystallographic directions must be taken into account. However, the rather large demagnetization factor $N \approx 0.3$ has only a negligible influence on the determination of $H_{c2}(T)$. Assuming that H_{c2} is defined at a susceptibility onset value $\chi_{ac}^* = -0.1$, then the actual value is only increased by about 3% if the demagnetization factor is taken into account. Assuming a superconducting transition width of ≈ 1 K, the shift (to higher values) of the critical temperature $T_c(H)$ for the determination of H_{c2} is less than 0.03 K. For some particular cases the H_{c2} values were also confirmed by resistive measurements. The magnetization of selected samples was measured as function of the applied magnetic field at constant temperature.

III. RESULTS AND DISCUSSIONS

Superconducting transition curves $\chi_{ac}(T)$ as function of the applied field $H \parallel [100]$ are shown in Fig. 1 for the $\text{Tb}_{0.2}\text{Y}_{0.8}\text{Ni}_2\text{B}_2\text{C}$ crystal as an example. The plots display a transition width of 0.8 K for $H=0$. With increasing magnetic field they exhibit a tail at low temperatures. From the $\chi_{ac}(T)$ plots H_{c2} values are derived by a tangent construction. In Fig. 2 the upper critical fields $H_{c2}(T)$ of a quaternary

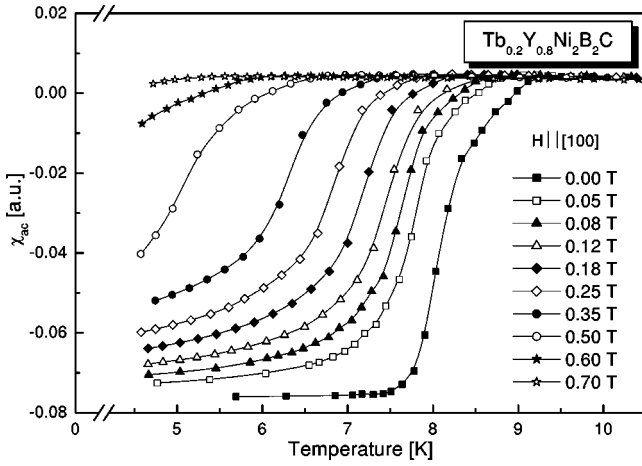


FIG. 1. ac susceptibility vs temperature plots $\chi_{ac}(T)$ as a function of external magnetic fields $H_{||}[100]$ for a $\text{Tb}_{0.2}\text{Y}_{0.8}\text{Ni}_2\text{B}_2\text{C}$ single crystal.

$\text{YNi}_2\text{B}_2\text{C}$ crystal and a pseudoquaternary $\text{Tb}_{0.1}\text{Y}_{0.9}\text{Ni}_2\text{B}_2\text{C}$ crystal are compared. In accordance with Ref. 8 we revealed an anisotropy $H_{c2}^{[001]} < H_{c2}^{[100]}$ for $\text{YNi}_2\text{B}_2\text{C}$ which is small but clearly visible for all considered temperatures T . By substituting 10% Tb for Y the magnitude of $H_{c2}(T)$ has been reduced, and there is a striking change of the anisotropy for $T < 10$ K: $H_{c2}^{[001]} > H_{c2}^{[100]}$. For $T > 10$ K the slight anisotropy $H_{c2}^{[001]} < H_{c2}^{[100]}$ is maintained. Similar to the case of $\text{YNi}_2\text{B}_2\text{C}$ the $H_{c2}(T)$ plots of the $\text{Tb}_{0.1}\text{Y}_{0.9}\text{Ni}_2\text{B}_2\text{C}$ single crystal display a positive curvature near T_c , which was previously explained by an effective two-band model.¹³ However, the shape of $H_{c2}(T)$ is changed, in particular, the range of quasilinear slope is reduced.

Increasing the concentration of Tb ions in $\text{Tb}_{0.2}\text{Y}_{0.8}\text{Ni}_2\text{B}_2\text{C}$ crystals, evidently enhances the anisotropy of upper critical fields, as shown in Fig. 3. The magnitude of $H_{c2}(T)$ is further reduced, approaching maximum values of $\mu_0 H_{c2}^{[001]}(2 \text{ K}) = 1.4 \text{ T}$ and $\mu_0 H_{c2}^{[100]}(2 \text{ K}) = 0.8 \text{ T}$, re-

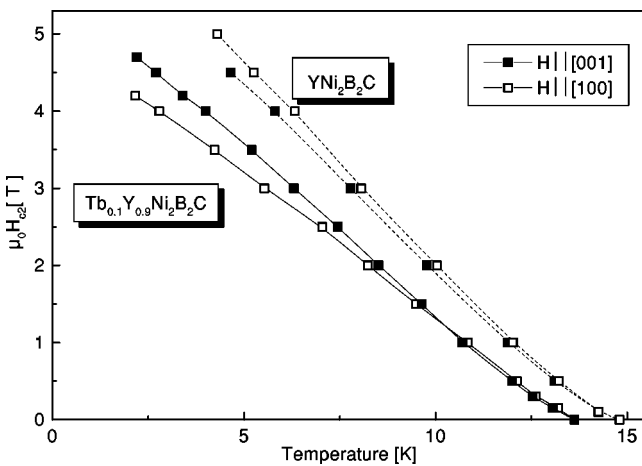


FIG. 2. Upper critical fields $H_{c2}^{[100]}(T)$ and $H_{c2}^{[001]}(T)$ as functions of temperature for $\text{YNi}_2\text{B}_2\text{C}$ and $\text{Tb}_{0.1}\text{Y}_{0.9}\text{Ni}_2\text{B}_2\text{C}$ single crystals with the orientations parallel to the a axis and the c axis, respectively.

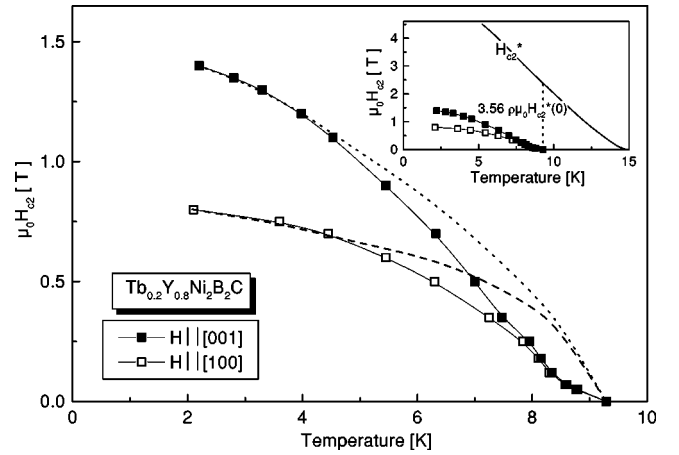


FIG. 3. Upper critical fields $H_{c2}^{[100]}(T)$ and $H_{c2}^{[001]}(T)$ as functions of temperature of a $\text{Tb}_{0.2}\text{Y}_{0.8}\text{Ni}_2\text{B}_2\text{C}$ single crystal for orientations parallel to the a axis and the c axis, respectively. The theoretical $H_{c2}(T)$ curves [Eq. (2)] are plotted as dotted ($H_{||}[001]$) and dashed ($H_{||}[100]$) lines. For comparison H_{c2}^* of the hypothetical nonmagnetic compound used in Eq. (2) is shown in the inset. The temperature independent reduction $3.56\rho\mu_0 H_{c2}^*(0)$ [third term in Eq. (2)] of H_{c2}^* , caused by scattering on the magnetic moments, is indicated.

spectively. The positive initial curvature of $H_{c2}(T)$ near T_c is retained. However, the $H_{c2}(T)$ plots exhibit no extended quasilinear regions. Instead, $H_{c2}(T)$ levels off near $T = 2$ K. With rising x the magnitude of the upper critical fields $H_{c2}^{[001]}$ and $H_{c2}^{[100]}$ further slopes down, as shown in Fig. 4, but the anisotropy in $\text{Tb}_{0.3}\text{Y}_{0.7}\text{Ni}_2\text{B}_2\text{C}$ and $\text{Tb}_{0.4}\text{Y}_{0.6}\text{Ni}_2\text{B}_2\text{C}$ single crystals is reduced in comparison with $\text{Tb}_{0.2}\text{Y}_{0.8}\text{Ni}_2\text{B}_2\text{C}$. For comparison the upper critical field in the diagonal direction in the basal plane $H_{c2}^{[110]}$ of the $\text{Tb}_{0.3}\text{Y}_{0.7}\text{Ni}_2\text{B}_2\text{C}$ crystal is presented in Fig. 4, which proves that the in-plane anisotropy is small.

It should be noted that the drop in T_c of the $\text{Tb}_x\text{Y}_{1-x}\text{Ni}_2\text{B}_2\text{C}$ crystals does not show a plain linear depen-

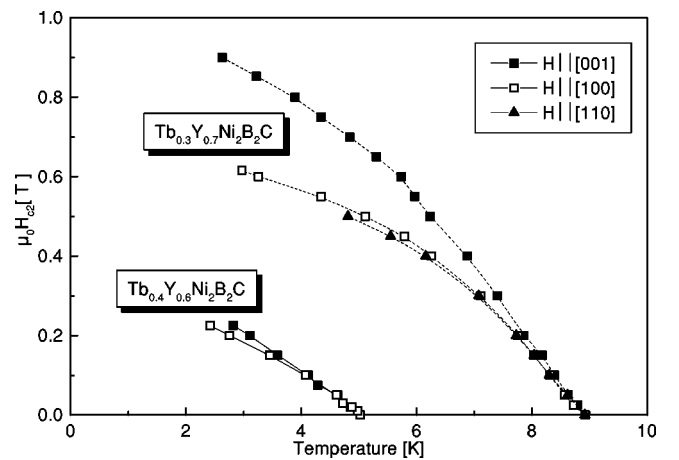


FIG. 4. Upper critical fields $H_{c2}^{[100]}(T)$ and $H_{c2}^{[001]}(T)$ vs temperature of $\text{Tb}_{0.3}\text{Y}_{0.7}\text{Ni}_2\text{B}_2\text{C}$ and $\text{Tb}_{0.4}\text{Y}_{0.6}\text{Ni}_2\text{B}_2\text{C}$ single crystals for orientations parallel to the a axis and the c axis, respectively. For comparison, $H_{c2}^{[110]}(T)$ of $\text{Tb}_{0.3}\text{Y}_{0.7}\text{Ni}_2\text{B}_2\text{C}$ is shown.

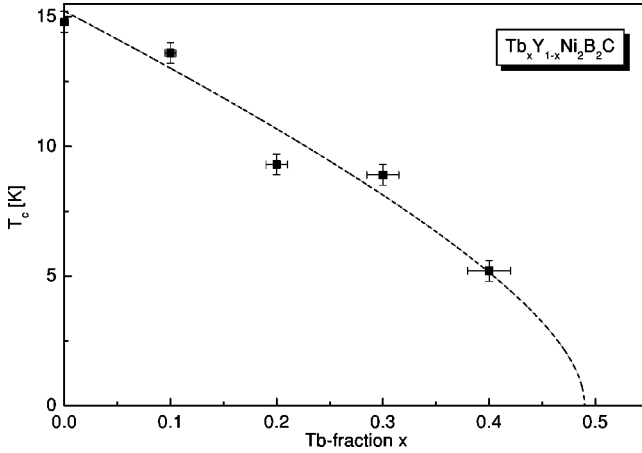


FIG. 5. Superconducting transition temperatures of $\text{Tb}_x\text{Y}_{1-x}\text{Ni}_2\text{B}_2\text{C}$ single crystals vs the Tb fraction x . The dashed line represents the fit according to the Abrikosov-Gor'kov theory [Eq. (1)].

dence on the Tb concentration x as compared to earlier results on polycrystalline samples⁶ and on single-crystalline samples grown by the flux technique.¹⁴ In particular, the difference in T_c for $x=0.2$ (9.3 K) and $x=0.3$ (8.9 K) is smaller than expected from the interpolated $T_c(x)$ plot (Fig. 5). Therefore, we expect that a slight shift of the Ni/B ratio within the homogeneity range of the intermetallic compound might be responsible for this deviation in superconducting properties. Such a phenomenon was already observed in $\text{HoNi}_2\text{B}_2\text{C}$ by Schmidt *et al.*¹⁵

In any case the upper critical fields $H_{c2}(T)$ of $\text{Tb}_x\text{Y}_{1-x}\text{Ni}_2\text{B}_2\text{C}$ compounds exhibit a monotonic rise with decreasing temperature. Furthermore, the extended linear range of $H_{c2}(T)$ and the positive curvature of $H_{c2}(T)$ near T_c , which are very pronounced in $\text{YNi}_2\text{B}_2\text{C}$, were reduced with increasing Tb content x and vanish for $x=0.4$.

The question arises of whether the observed features of $\text{Tb}_x\text{Y}_{1-x}\text{Ni}_2\text{B}_2\text{C}$ crystals, especially the anomalous large anisotropy of the upper critical field H_{c2} , are caused by the interaction of conduction electrons with the magnetic moments of the R ions. The density of states at the Fermi level in $\text{YNi}_2\text{B}_2\text{C}$ is mainly governed by the Ni-derived $3d$ states,¹⁶ but there is also a significant contribution of R $4d$ and R $5p$ electrons to the Fermi surface.¹⁷ Therefore, an effect of the magnetic moments on the conduction electrons, mediated by exchange interaction, is expected. In a first approximation this exchange interaction can be considered as some effective field. This view is supported by the fact that some characteristics of $\text{YNi}_2\text{B}_2\text{C}$, which are due to special features of the Fermi surface, e.g., the positive curvature of $H_{c2}(T)$ near T_c , are retained in $\text{Tb}_x\text{Y}_{1-x}\text{Ni}_2\text{B}_2\text{C}$ crystals whereas the sign of the anisotropy is inverted. Therefore, we suspected that the interaction of magnetic Tb ions with conduction electrons is not only responsible for the sizable reduction of the upper critical field but also governs the anisotropy of $H_{c2}(T)$.

Field-dependent magnetization measurements of the $\text{Tb}_{0.2}\text{Y}_{0.8}\text{Ni}_2\text{B}_2\text{C}$ single crystals which display the largest $H_{c2}(T)$ anisotropy have been performed at selected tempera-

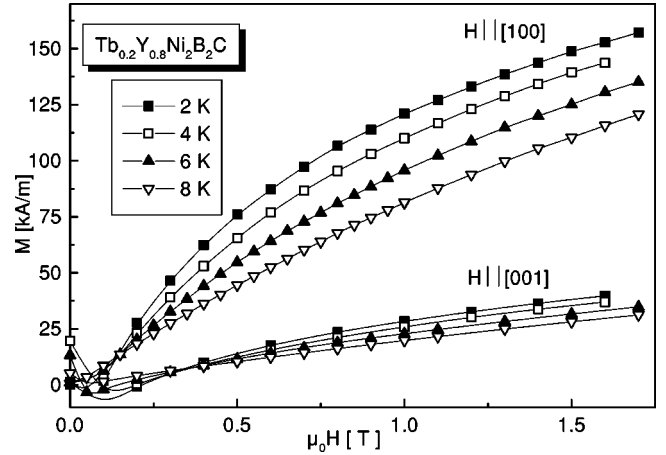


FIG. 6. Magnetization M vs external field H of $\text{Tb}_{0.2}\text{Y}_{0.8}\text{Ni}_2\text{B}_2\text{C}$ for orientations $H||[100]$ and $H||[001]$ at selected temperatures $T=2-8$ K.

tures. They revealed a considerably higher in-plane magnetization for $H||[100]$ than the magnetization for $H||[001]$ (Fig. 5). That is, the anisotropy of the spin configuration of $\text{TbNi}_2\text{B}_2\text{C}$, characterized by magnetic moments within the tetragonal basal plane,¹⁸ is retained in $\text{Tb}_x\text{Y}_{1-x}\text{Ni}_2\text{B}_2\text{C}$. This is not surprising because the crystalline electric fields acting on the Tb ions should not be much affected by the dilution with Y. This leads to an enhanced effective magnetic field for $H||[100]$ which interacts with the superconducting electrons and finally reduces the critical field H_{c2} . The fact that there is practically no in-plane anisotropy of $H_{c2}(T)$ in $\text{Tb}_{0.3}\text{Y}_{0.7}\text{Ni}_2\text{B}_2\text{C}$ (compare Fig. 4) is consistent with previously reported magnetization measurements in some dilute $\text{Tb}_x\text{Y}_{1-x}\text{Ni}_2\text{B}_2\text{C}$ compounds which exhibit a nearly isotropic in-plane magnetization.¹⁹

A quantitative relationship between the measured H_{c2} and the magnetization can be developed on the basis of the Abrikosov-Gor'kov theory. For the pseudoquaternary borocarbides $R_xR'_{1-x}\text{Ni}_2\text{B}_2\text{C}$ the effect of partial substitution of the R -sites by *magnetic* rare-earth ions on the upper critical field, to the best of our knowledge has not been studied so far. As shown in Fig. 6 in the present case for $\text{Tb}_x\text{Y}_{1-x}\text{Ni}_2\text{B}_2\text{C}$ the usual Abrikosov-Gor'kov dependence

$$\ln(T_c^0/T_c) = \psi\left(\frac{1}{2} + \frac{T_c^0\rho}{2T_c(x)}\right) - \psi\left(\frac{1}{2}\right) \quad (1)$$

holds in principle, where $\rho \approx 0.76x$ is the pair-breaking parameter obtained from the fit of our $T_c(x)$ data. The Abrikosov-Gor'kov theory only describes the effect of paramagnetic impurities on superconductivity. However, there may be additional effects on superconducting properties due to a variable sample composition within the homogeneity range of the $R_xR'_{1-x}\text{Ni}_2\text{B}_2\text{C}$ intermetallic compounds which are not reflected by the Abrikosov-Gor'kov approach. This has been shown exemplary for the $\text{Tb}_x\text{Er}_{1-x}\text{Ni}_2\text{B}_2\text{C}$ series where differences of T_c up to 2.5 K have been observed for samples with exactly the same Tb/Er ratio.²⁰

Since the observed anisotropy for $\text{YNi}_2\text{B}_2\text{C}$ presumably caused by the anisotropic Fermi surface is weak for a quantitative discussion we adopt an effective isotropic approach²¹ for a superconductor with paramagnetic impurities. This approach has been applied to closely related magnetic ternary rare-earth transition-metal compounds (e.g., ErRh_4B_4).²² Accordingly, the upper critical field can be written as

$$\begin{aligned} \mu_0 H_{c2}(T) = & \mu_0 H_{c2}^*(T) - \mu_0 M(H_{c2}, T) - 3.56\rho\mu_0 H_{c2}^*(0) \\ & - \frac{\alpha_M \lambda_{so}}{T_{c0}} [\mu_0 H_{c2}(T) + \mu_0 M(H_{c2}, T) \\ & + \mu_0 H_J(H_{c2}, T)]^2. \end{aligned} \quad (2)$$

The Maki parameter α_M is defined by the well-known relation

$$\alpha_M = \sqrt{2} H_{c2}^*(0) / H_{p0}, \quad (3)$$

where $H_{c2}^*(0) = H_{c2}^*(x=0, T=0)$ is the extrapolated orbital critical field at zero temperature of the pure stoichiometric superconductor without magnetic impurities, and H_{p0} is the paramagnetic limiting field which in the BCS limit reads

$$H_{p0} = 1.84 T_c \text{ [K]} = 27.2 \text{ T}. \quad (4)$$

In the same approach the relation between the total (measured) upper critical field H_{c2} and the orbital one H_{c2}^* reads

$$H_{c2}^*(0) = H_{c2}(0) / [1 - H_{c2}(0) / H_{p0}] \approx 11.7 \text{ T}, \quad (5)$$

where $H_{c2}(0) \approx 8.2 \text{ T}$ has been estimated. Then with these estimated values we arrive finally at $\alpha_M = 0.607 \approx 0.61$. The quantity $\lambda_{so} = 1$ denotes a typical value of the spin-orbit coupling constant, and $T_{c0} = 14.8 \text{ K}$ is the critical temperature without magnetic impurities. Finally, for the case without magnetic impurities for the sake of simplicity all field are assumed to be isotropic.

With the experimental data of $H_{c2}(T)$ and the $M(H)$ curves of $\text{Tb}_{0.2}\text{Y}_{0.8}\text{Ni}_2\text{B}_2\text{C}$ and the upper critical field of $\text{YNi}_2\text{B}_2\text{C}$ the local exchange field H_J can be estimated for both $H \parallel [100]$ and $H \parallel [001]$. At 2 K we obtain $\mu_0 H_J^{[100]}(2 \text{ K}) = 1.5 \text{ T}$ and $\mu_0 H_J^{[001]}(2 \text{ K}) = 0.5 \text{ T}$. It is interesting to note that the latter field is similar in magnitude to the threshold fields of metamagnetic transitions in $\text{TbNi}_2\text{B}_2\text{C}$, 1.5 and 2.5 T, for $H \perp [001]$.^{23,24} As the local exchange field is proportional to the magnetization, $H_J(T)$ can be calculated for the whole temperature range investigated. With these data based on Eq. (2), the theoretical $H_{c2}(T)$ curves have been calculated for both directions which are shown in Fig. 3 as dashed and dotted lines. A comparison with the experimental data reveals that the theoretical values fit the experimental data well for low temperatures (where the parameter H_J has been determined). The

results apparently reflect the anisotropy of $H_{c2}(T)$ for the $[001]$ and $[100]$ directions, respectively, which is caused by the magnetic moments of the Tb ions. The simple approach fails to describe the $H_{c2}(T)$ plots if the critical temperature T_c is approached. In particular, the plain one-band model applied is not able to reproduce the experimentally observed positive curvature of $H_{c2}(T)$. A theoretical two-band model which well describes the positive curvature of H_{c2} was recently presented for nonmagnetic compounds like $\text{YNi}_2\text{B}_2\text{C}$.¹³ However, a more sophisticated two-band model involving magnetic effects, which can reproduce all features of the $H_{c2}(T)$ plots, is still a challenge for future theoretical work.

The increasing fraction of Tb ions leads to a rising anisotropy of the upper critical field up to $x=0.2$. For $x>0.2$ the anisotropy again declines. This may be explained by magnetic ordering of Tb ions, suggested by specific heat measurements which display a peak due to a magnetic ordering transition in $\text{Tb}_{0.3}\text{Y}_{0.7}\text{Ni}_2\text{B}_2\text{C}$ ($T_N=3.6 \text{ K}$) and $\text{Tb}_{0.4}\text{Y}_{0.6}\text{Ni}_2\text{B}_2\text{C}$ ($T_N=5.2 \text{ K}$) single crystals.²⁵ In the case of $\text{TbNi}_2\text{B}_2\text{C}$ temperature-dependent magnetization measurements have revealed that the transition from paramagnetic to antiferromagnetic ordering leads to a higher reduction of M for $H \perp [001]$ than for $H \parallel [001]$.²⁶ This might explain the decrease of the $H_{c2}(T)$ anisotropy for higher Tb fractions ($x \geq 0.3$).

IV. SUMMARY

To summarize, we have shown that the anisotropic magnetization is a key quantity which determinates the anisotropic upper critical fields in rare earth-transition-metal borocarbides containing paramagnetic impurities. The theory of Fischer, which is strictly valid for *dirty limit* superconductors, leads to reasonable quantitative results even for the *clean limit* borocarbides. We may conclude that the $H_{c2}(T)$ anisotropy of the pseudoquaternary compounds mainly results from the polarization of the conduction electron spin [the fourth term in Eq. (2)]. The local exchange field H_J which exceeds the magnetization M by roughly one order of magnitude has been revealed as the decisive quantity. The magnitude of the anisotropy is governed both by the fraction x of Tb ions and magnetic ordering effects. This series of $\text{Tb}_x\text{Y}_{1-x}\text{Ni}_2\text{B}_2\text{C}$ single crystals represents a prominent example how the anisotropy of superconductivity can be tuned by the strength of magnetic interaction.

ACKNOWLEDGMENTS

This work was performed with financial support of the DFG within SFB 463 ‘‘Rare-earth intermetallics: Structure, Magnetism and Transport.’’ Discussions with S.V. Shulga, A. Morozov, and M. Divis are gratefully acknowledged.

*Corresponding author. Email address: w.loeser@ifw-dresden.de

[†]On leave from International Laboratory of High Magnetic Fields, Wroclaw, Poland

¹R. Nagarajan, C. Mazumdar, Z. Hossain, S. K. Dhar, K. V.

Gopalakrishnan, L. C. Gupta, C. Godart, B. D. Padalia, and R. Vijayaraghavan, Phys. Rev. Lett. **72**, 274 (1994).

²R. J. Cava, H. Takagi, H. W. Zandbergen, J. J. Krajewski, W. F. Peck, Jr., T. Siegrist, B. Batlogg, R. B. van Dover, R. J. Felder,

- K. Mizuhashi, J. O. Lee, and S. Uchida, *Nature (London)* **367**, 252 (1994).
- ³M. Xu, P. C. Canfield, J. E. Ostenson, D. K. Finnemore, B. K. Cho, Z. R. Wang, and D. C. Johnston, *Physica C* **227**, 321 (1994).
- ⁴B. K. Cho, P. C. Canfield, and D. C. Johnston, *Phys. Rev. Lett.* **77**, 163 (1996).
- ⁵K. Eversmann, A. Handstein, G. Fuchs, L. Cao, and K. H. Müller, *Physica C* **266**, 27 (1996).
- ⁶H. Bitterlich, W. Löser, G. Behr, K. Nenkov, G. Fuchs, A. Belger, and L. Schultz, *Physica C* **308**, 243 (1998).
- ⁷P. C. Canfield, P. L. Gammel, and D. J. Bishop, *Phys. Today* **52** (10), 40 (1998).
- ⁸H. Takagi, M. Nohara, and R. J. Cava, *Physica B* **237-238**, 292 (1997).
- ⁹A. C. DuMar, K. D. Rathnajaka, D. G. Naugle, and P. C. Canfield, *Int. J. Mod. Phys. B* **12**, 3264 (1998).
- ¹⁰P. Dervenagas, J. Zaretsky, C. Stassis, A. I. Goldman, P. C. Canfield, and B. K. Cho, *Phys. Rev. B* **53**, 8506 (1996).
- ¹¹H. Bitterlich, W. Löser, G. Behr, G. Graw, W. Yang-Bitterlich, U. Krämer, and L. Schultz, *J. Cryst. Growth* **213**, 319 (2000).
- ¹²G. Behr, W. Löser, G. Graw, K. Nenkov, U. Krämer, A. Belger, and B. Wehner, *J. Mater. Res.* **14**, 16 (1999).
- ¹³S. V. Shulga, S.-L. Drechsler, G. Fuchs, K.-H. Müller, K. Winzer, M. Heinecke, and K. Krug, *Phys. Rev. Lett.* **80**, 1730 (1998).
- ¹⁴B. K. Cho, H. B. Kim, and S. I. Lee, *Phys. Rev. B* **63**, 144528 (2001).
- ¹⁵H. Schmidt, M. Weber, and H. F. Braun, *Physica C* **246**, 177 (1995).
- ¹⁶L. F. Mattheis, *Phys. Rev. B* **49**, 13 279 (1994).
- ¹⁷M. Divis, K. Schwarz, P. Blaha, G. Hilscher, H. Michor, and S. Khmelevskiy, *Phys. Rev. B* **62**, 6774 (2000).
- ¹⁸B. K. Cho, P. C. Canfield, and D. C. Johnston, *Phys. Rev. B* **53**, 8499 (1996).
- ¹⁹H. Bitterlich, W. Löser, K. Nenkov, G. Fuchs, K. Winzer, and L. Schultz, *Physica B* **284-288**, 487 (2000).
- ²⁰H. Bitterlich, W. Löser, G. Behr, K. Nenkov, G. Fuchs, A. A. Gümbel, and L. Schultz, *Physica C* **321**, 93 (1999).
- ²¹Ø. Fischer, in *Ferromagnetic Materials*, edited by K. H. J. Buschow and E. P. Wohlfarth (Elsevier, Amsterdam, 1990), p. 466.
- ²²H. Iwasaki and Y. Muto, *Phys. Rev. B* **33**, 4680 (1986).
- ²³P. C. Canfield and S. L. Budko, *J. Alloys Compd.* **262-263**, 196 (1997).
- ²⁴K. H. Müller, A. Handstein, D. Eckert, G. Fuchs, K. Nenkov, J. Freudenberger, M. Richter, and M. Wolf, *Physica B* **246-247**, 226 (1996).
- ²⁵H. Michor (private communication).
- ²⁶C. V. Tomy, L. A. Afalfiz, M. R. Lees, J. M. Martin, D. McK. Paul, and D. T. Adroja, *Phys. Rev. B* **53**, 307 (1996).